23rd International Conference on
Harmonisation within Atmospheric Dispersion Modelling
for Regulatory Purposes
15-19 September 2025, Hamburg, Germany

EXTENDED ABSTRACT

Abstract title: Automatization of mesh generation from point cloud 3D scans to model the surface atmospheric boundary layer.

Name and Affiliation of the First Author: **Mahitosh Mehta**; CEREA, École nationale des ponts et chaussées, EDF R&D, Champs-sur-Marne, France.

Email of first author: mahitosh.mehta@enpc.fr

Names and Affiliations of the Co-authors: **Martin Ferrand**; CEREA, École nationale des ponts et chaussées, Champs-sur-Marne, France; EDF R&D, 6, quai Watier, 78400 Chatou, France. **Samuel Gaucher**; EDF R&D, 6, quai Watier, 78400 Chatou, France.

Introduction

Handling intricate geometries in industrial computational fluid dynamics (CFD) simulations present significant challenges. However, advancements in 3D scanning technologies now enable the detailed capture of highly complex structures for use in CFD models. The study presented in this paper introduces the use of a new methodology for automatically reconstructing solid geometries from 3D scan data (Narváez et al. 2023) integrating them into flow simulations. Starting from a 3D point cloud, the method rebuilds the solid surface by identifying and incorporating local planar regions within each convex computational cell. There exist other methods in literature for surface reconstruction such as by interpolation parametric surfaces (Hoppe et al. 1992; Amenta et al. 2001; Kazhdan et al. 2006) or through a signed scalar function (Bouchiba et al. 2020; Kovalčíková Ďuračíková et al. 2022).

From the numerical modelling point of view, the approaches for representing solids in contact with fluids can be classified into the body-fitted methods (BFM) and immersed boundary methods (IBM). The classic body-fitted mesh paradigm consists in removing the solid domain from the mesh and imposing the boundary conditions directly on the mesh boundary, whereas in IBM, the solid is embedded inside the fluid mesh and the boundary conditions are imposed at the fluid-solid interface inside the mesh within a co-located finite volume framework. This strategy eliminates the need for the traditionally labour-intensive and time-consuming body-fitted meshing process, while maintaining good accuracy and computational robustness.

As the aim of this work is to develop an automatic framework to apply a point cloud to simulate fluid dynamics directly, it is a crossroad of multiple scientific domains, including immersed boundary computational fluid dynamics and geometry processing. In the following sections we discuss the surface reconstruction and surface orientation algorithms, and their application to point clouds obtained for the site of Sirta.

Fluid domain and solid surface reconstruction Algorithm for fluid simulation from point cloud on solid surface orientation

In this work, we propose an algorithm to identify the correct plane orientation to identify between solid and fluid regions. Computationally, surfaces can be represented using various methods, broadly categorized into explicit and implicit representations. Explicit representations include point clouds (sets of points on a surface) or a set of triangles connecting these points. In contrast, implicit representations define a surface as the level set of a scalar function.

Surface reconstruction is a key process in these fields, transforming a set of points into a continuous surface. A detailed survey by (Berger et al. 2014) explores various surface reconstruction techniques. Explicit reconstruction methods typically involve interpolating point clouds to form surfaces (Bernardini et al. 1999). However, these methods may struggle with noisy or complex real-world point clouds. Implicit reconstruction, on the other hand, often constructs a signed distance function from the data (Curless and Levoy 1996; Mullen et al. 2010), where the surface is defined by the function's zero level set. This approach can also be framed as solving a Poisson equation using oriented normal (Kazhdan et al. 2006; Kazhdan and Hoppe 2013). Notably, (Alliez et al. 2007) proposed a method that bypasses the need for oriented normals.

Some techniques bridge implicit and explicit representations by generating explicit surfaces from implicit scalar functions, such as distance fields (Lorensen and Cline 1998; Schaefer and Warren 2004; Treece et al. 1999). Recently, (Bouchiba et al. 2020) introduced an implicit scalar function defined across the entire computational domain, enabling its use in immersed boundary fluid simulations within finite element solvers.

The algorithm used here to reconstruct the surface takes a hybrid approach by leveraging data points within a cell to form a plane that reduces the mean square error to its minimum. This plane acts as an implicit definition of the surface and is later applied explicitly to compute essential geometric characteristics of the cell or its face. These characteristics include the volume, surface area, and centre of gravity of the fluid portion. For further explanation on the algorithm for surface reconstruction the reader is advised to refer to (Narváez et al. 2023). However, this method calls for correctly oriented normals.

Initial filling of a fluid domain

There are two algorithms developed to extract the solid domain from the computational domain.

- an approach based on the porosity gradient and the source of the scan, here after called "Radial fill".
- an approach based on pure convection using a direction vector, here after called "Directional fill".

The "Radial fill" approach was developed previously and explained in detail by (Narváez et al. 2023). The point cloud we use here is obtained by a LiDAR scan which is carried out using drones. To simulate the behaviour of this scan, the development of a new algorithm is necessary, which is explained in detail below.

The algorithm "Radial fill" numerically reproduces what a scanner does: from a point source where the scanner is located, numerical rays are traced in all directions (like the Discrete Ordinate Method to solve the radiative transfer equation). It corresponds to a steady pure convection equation on ψ, whose continuous (first line) and discrete formulations (second line) are, respectively:

$$\nabla\psi \cdot (x - x_0) = (1 - \psi)\,\delta_{x_0}(x)$$

$$\sum_{f \in F_c} [\psi_f - \psi_c](x_f - x_0) \cdot S_{fc}^{\psi,0} = (1 - \psi_c)\,\Omega_c 1_{x_0 \in c}$$

Unlike ray-casting-based formulations which trace fill from a point source outward, for "Directional fill" we model scalar transport as a directional flux propagating from a known inflow boundary (e.g., the top of the domain) downward as presented in Figure 1. For this approach, a steady pure convection equation on ψ can be written as following in the fluid region with Dirichlet boundary condition at the top:

$$\nabla\psi \cdot d = 0$$

$$\sum_{f \in F_c} [\psi_f - \psi_c] d \cdot S_{fc}^{\psi,0} = 0$$

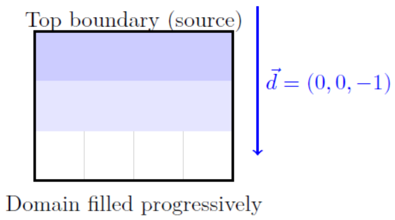

Figure **1**: top-down pure convection fill process. Fill is injected at the top boundary and propagates in the direction **d.**

with $x_0$being the source position, d being the fixed convection direction and the indicator function $1_{x_0 \in c} = \int_c \delta_{x_0}(x) d\psi$ if the cell contains the source, and zero otherwise. The scalar at the faces ψ_f is estimated by an upwind scheme. Cells with more than three scan points are penalised and stop the rays (i.e., are fully solid cells with $S_{fc}^{\psi,0} = 0$). Thus, ψ fills the fluid domain ($\psi = 1$ for fluid and $\psi = 0$ for solid). As many loops as available scans are performed, storing the maximum of ψ. If ψ bigger than one-half, the cell is considered fluid. It means that $\nabla_c\psi$ points towards the fluid region in solid cells in contact with the fluid.

This directional fill formulation enables efficient propagation of fill from the inflow boundary without requiring ray-tracing or distance computations. It is particularly well-suited for applications where the fill direction is uniform and known a priori, such as gravity-driven flooding or downward expansion in immersed boundary reconstruction. The use of the saturation term $(1 - \psi)$ preserves monotonicity and ensures that filled regions remain stable once filled. Note that $S_{fc}^{\psi,0}$ is the fluid face first guess to run the orientation algorithm. However, considering that cells with a solid plane (i.e., with scan points) are split into solid and fluid parts, the fluid cell and face geometric quantities are then updated using the deduced solid plane information.

Immersed plane orientation

The plane's normal orientation is essential to identify between solid and fluid regions. The definition of the normal orientation is not an easy task. This step is critical for accurately representing the geometry and physical behaviour at the interface between fluid and solid regions, such as in simulations involving immersed boundaries or porous media. To ensure that the normal vectors associated with cell faces are correctly oriented to point toward the solid region in a fluid-solid interaction model we developed an algorithm which gives the first approximation of the normal orientation by:

- temporarily enabling solid cells to compute the porosity gradient across the entire domain and determining the direction toward the solid region from that;
- flipping face normal vectors if they are misaligned with the porosity gradient or a specified direction vector (for directional filling);
- restoring the fluid-only computation mode by disabling solid cells.

Results

Airborne laser scanning system allows distance measurements to be made between a point on an aircraft and points on the ground, whose frequency domains can be in the visible or infrared range. Coupled with a scanning system, a GPS (Global Positioning System) and an inertial unit, it makes it possible to obtain a georeferenced point cloud during an acquisition. Under the national LiDAR HD program, the IGN (Institut national de l'information géographique et forestière) produces and disseminates a 3D map of the entire soil and surface of France in LiDAR data (IGN 2022). The resulting high-resolution point cloud data serves as input for surface reconstruction using code_saturne (Archambeau et al. 2004), an open-source CFD software developed by EDF. This process enables detailed simulations of atmospheric flows over complex terrains, supporting a range of environmental and engineering applications. Figures presented below illustrate key steps in the processing workflow. Figure 2 shows the generation of a solid plane from the point clouds (on right), based on the methodology described above, alongside the original point clouds (on left). Figure 3 presents the selected computational domain, represented by the computed distance to the ground, with the point clouds and their associated classifications in the background. The LiDAR dataset includes multiple classification types such as building, bridges, vegetation, etc., each assigned a specific numerical value. The algorithm described above require further testing using the point clouds of different sites. The Ongoing work focuses on filling of the holes caused by the missing information in the LiDAR data (one of the major defects in point clouds), and adding the source terms to the cells containing vegetation, in order to simulate conditions as closely as possible to the real environment.

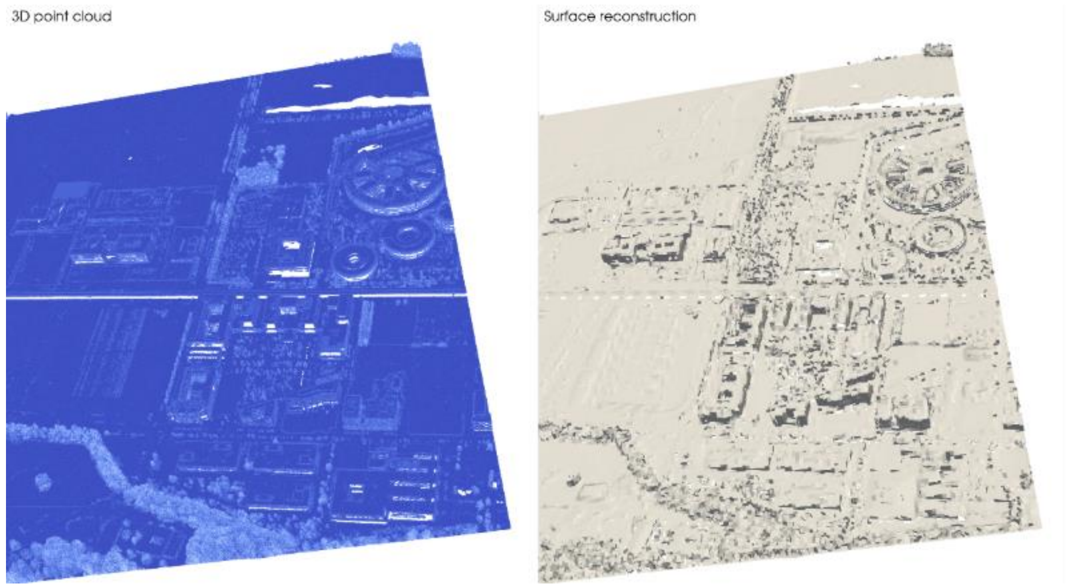

Figure 2: representation of solid reconstruction from 3D scan point cloud of Sirta.

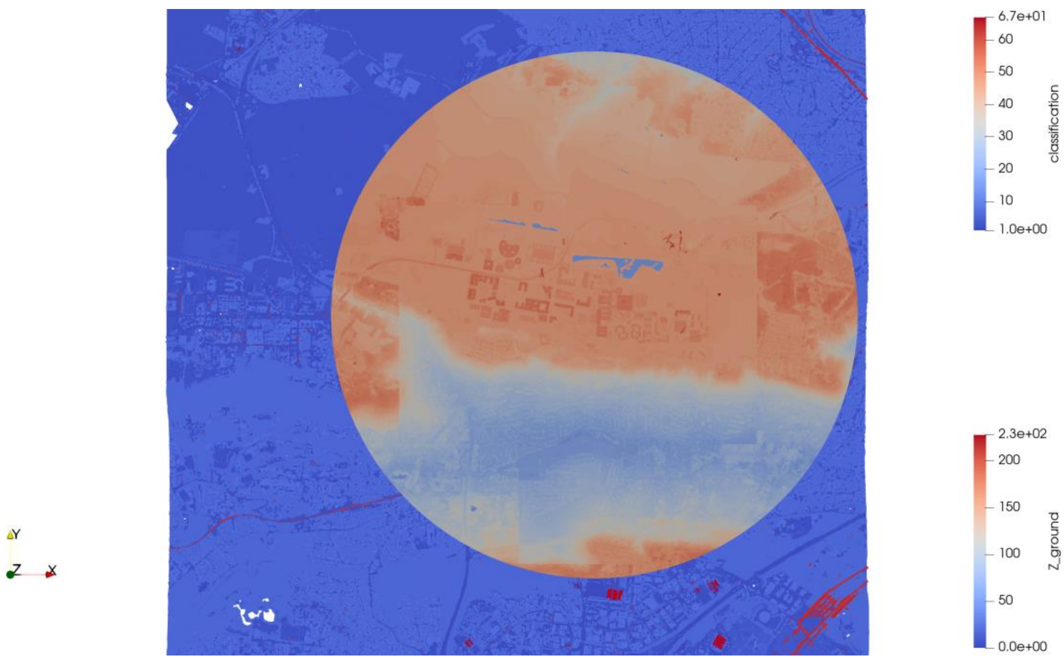

Figure 3: representation of the computed distance to the ground (z_ground) in the computational domain (represented by the circular disk) with point clouds in the background for the site of Sirta.

Bibliography

Alliez, P., D. Cohen-Steiner, Y. Tong, and M. Desbrun. 2007. 'Voronoi-Based Variational Reconstruction of Unoriented Point Sets'. *Proceedings of the Fifth Eurographics Symposium on Geometry Processing* (Goslar, DEU), SGP '07, July 4, 39–48.

Amenta, Nina, Sunghee Choi, and Ravi Krishna Kolluri. 2001. 'The Power Crust'. *Proceedings of the Sixth ACM Symposium on Solid Modeling and Applications* (New York, NY, USA), SMA '01, May 1, 249–66. https://doi.org/10.1145/376957.376986.

Archambeau, Frédéric, Namane Méchitoua, and Marc Sakiz. 2004. 'Code Saturne: A Finite Volume Code for the Computation of Turbulent Incompressible Flows - Industrial Applications'. *International Journal on Finite Volumes* 1 (1): http://www.latp.univ-mrs.fr/IJFV/spip.php?article3.

Berger, Matthew, Andrea Tagliasacchi, Lee Seversky, et al. 2014. 'State of the Art in Surface Reconstruction from Point Clouds'. 1 (1): 161. https://doi.org/10.2312/egst.20141040.

Bernardini, F., J. Mittleman, H. Rushmeier, C. Silva, and G. Taubin. 1999. 'The Ball-Pivoting Algorithm for Surface Reconstruction'. *IEEE Transactions on Visualization and Computer Graphics* 5 (4): 349–59. https://doi.org/10.1109/2945.817351.

Bouchiba, Hassan, Simon Santoso, Jean-Emmanuel Deschaud, Luisa Rocha-Da-Silva, François Goulette, and Thierry Coupez. 2020. 'Computational Fluid Dynamics on 3D Point Set Surfaces'. *Journal of Computational Physics: X* 7 (June): 100069. https://doi.org/10.1016/j.jcpx.2020.100069.

Curless, Brian, and Marc Levoy. 1996. 'A Volumetric Method for Building Complex Models from Range Images'. *Proceedings of the 23rd Annual Conference on Computer Graphics and Interactive Techniques* (New York, NY, USA), SIGGRAPH '96, August 1, 303–12. https://doi.org/10.1145/237170.237269.

Hoppe, Hugues, Tony DeRose, Tom Duchamp, John McDonald, and Werner Stuetzle. 1992. 'Surface Reconstruction from Unorganized Points'. *Proceedings of the 19th Annual Conference on Computer Graphics and Interactive Techniques* (New York, NY, USA), SIGGRAPH '92, July 1, 71–78. https://doi.org/10.1145/133994.134011.

IGN. 2022. 'Documentation on LiDAR HD – Version 1.0'. https://geoservices.ign.fr/sites/default/files/2024-09/DC_LiDAR_HD_1-0.pdf.

Kazhdan, Michael, Matthew Bolitho, and Hugues Hoppe. 2006. 'Poisson Surface Reconstruction'. *Proceedings of the Fourth Eurographics Symposium on Geometry Processing* (Goslar, DEU), SGP '06, June 26, 61–70.

Kazhdan, Michael, and Hugues Hoppe. 2013. 'Screened Poisson Surface Reconstruction'. *ACM Trans. Graph.* 32 (3): 29:1-29:13. https://doi.org/10.1145/2487228.2487237.

Kovalčíková Ďuračíková, Kristína, Alžbeta Bugáňová, and Ivan Cimrák. 2022. 'Modelling of Arbitrary Shaped Channels and Obstacles by Distance Function'. In *Bioinformatics and Biomedical Engineering*, edited by Ignacio Rojas, Olga Valenzuela, Fernando Rojas, Luis Javier Herrera, and Francisco Ortuño. Springer International Publishing. https://doi.org/10.1007/978-3-031-07704-3_3.

Lorensen, William E., and Harvey E. Cline. 1998. 'Marching Cubes: A High Resolution 3D Surface Construction Algorithm'. In *Seminal Graphics: Pioneering Efforts That Shaped the Field, Volume 1*, Volume 1. Association for Computing Machinery. https://doi.org/10.1145/280811.281026.

Mullen, Patrick, Fernando De Goes, Mathieu Desbrun, David Cohen-Steiner, and Pierre Alliez. 2010. 'Signing the Unsigned: Robust Surface Reconstruction from Raw Pointsets'. *Computer Graphics Forum* 29 (5): 1733–41. https://doi.org/10.1111/j.1467-8659.2010.01782.x.

Narváez, Gabriel F., Martin Ferrand, Thomas Fonty, and Sofiane Benhamadouche. 2023. 'Automatic Solid Reconstruction from 3-D Points Set for Flow Simulation via an Immersed Boundary Method'. In *Finite Volumes for Complex Applications X—Volume 1, Elliptic and Parabolic Problems*, edited by Emmanuel Franck, Jürgen Fuhrmann, Victor Michel-Dansac, and Laurent Navoret. Springer Nature Switzerland. https://doi.org/10.1007/978-3-031-40864-9_30.

Schaefer, S., and J. Warren. 2004. 'Dual Marching Cubes: Primal Contouring of Dual Grids'. *12th Pacific Conference on Computer Graphics and Applications, 2004. PG 2004. Proceedings.*, October, 70–76. https://doi.org/10.1109/PCCGA.2004.1348336.

Treece, G. M., R. W. Prager, and A. H. Gee. 1999. 'Regularised Marching Tetrahedra: Improved Iso-Surface Extraction'. *Computers & Graphics* 23 (4): 583–98. https://doi.org/10.1016/S0097-8493(99)00076-X.